EFFECTS OF POROUS SUPERHYDROPHILIC SURFACES ON FLOW BOILING CRITICAL HEAT FLUX IN IVR ACCIDENT SCENARIOS

Reza Azizian[1], Thomas McKrell[1], Kresna Atkhen[2], and Jacopo Buongiorno[1]
[1]Nuclear Science and Engineering Department, Massachusetts Institute of Technology, Cambridge, 02139, USA
Azizian@mit.edu; Tmckrell@mit.edu; Jacopo@mit.edu
[2]*Électricité de France* (EDF)-R&D, France
Kresna.atkhen@edf.fr

Abstract
Critical Heat Flux (CHF) plays a key role in nuclear reactor safety both during normal operation as well as in accident scenarios. In particular, when an in-vessel retention (IVR) strategy is used as a severe accident management strategy, the reactor pressure vessel (RPV) cavity is flooded with water, to remove the decay heat from the corium relocated in the lower plenum by conduction through the RPV wall and flow boiling on the outer surface of the RPV. The CHF limit must not be exceeded to prevent RPV failure. Therefore, knowledge of the CHF under realistic conditions is necessary to assess coolability margins. Previous studies for prediction of CHF in the IVR situation were mostly based on data for as fabricated un-oxidized stainless steel. However, the RPV is made of low carbon steel and its surface has an oxide layer that results from pre-service heat treatment as well as oxidation during service. This oxide layer introduces significant differences in surface wettability, porosity, and roughness in comparison to an un-oxidized stainless steel surface. In this study, test heaters were fabricated out of RPV low carbon steel, pre-oxidized in a controlled high temperature wet air environment, which emulates the surface oxides present on the outer surface of the actual RPV; the heaters were then tested in a flow boiling loop designed specifically for the IVR conditions. Up to 70% enhancement in CHF value was observed for the oxidized in low carbon steel in comparison to the stainless steel.

Keywords: Critical heat flux, in-vessel retention, oxidation, superhydrophilic

1. Introduction

In-vessel retention (IVR) is a severe accident management strategy that is used in a number of modern nuclear power reactor designs, such as Westinghouse's AP1000. In the case of IVR, the reactor pressure vessel (RPV) cavity is flooded with water, so the decay heat from the molten fuel is removed by conduction through the RPV wall and flow boiling on the outer surface of the RPV. Flow boiling heat removal is limited by critical heat flux (CHF). Therefore increasing CHF provides a higher safety margin. There is mounting evidence that CHF in both pool boiling as well as flow boiling is sensitive to the characteristics of the boiling surface: this is in contrast to the earlier CHF models which ignored such effects.

In pool boiling, the separate effects of surface wettability, porosity, and roughness on pool boiling CHF in water were recently examined at MIT [1], using engineered surfaces. This experimental work showed that *porous hydrophilic* surfaces can enhance CHF by 50%-60%. In contrast *porous hydrophobic* surfaces resulted in a reduction of CHF by 97%. This study readily

showed the significance of surface characteristics on pool boiling CHF. Similar trends were also observed during the boiling of nanofluids. Precipitation of nanoparticles on the heater surface during nucleate boiling alters the surface characteristics of the boiling surface and provides a porous layer whose morphology depends on the nanoparticles. This porous layer was proposed as the reason for the observed enhancement in CHF of nanofluids boiling [2].

There are also several studies which explored the effect of surface characteristics on flow boiling CHF, a good review of which can be found in Ref. [3]. Given the importance of CHF in the IVR situation, many studies have also focused on different aspects of the IVR flow boiling CHF: the University of California, Santa Barbara (UCSB) [4-6], the SULTAN facility in France [7], the University of California, Los Angeles (UCLA) [8], the CYBL facility at Sandia [9], and Penn State University (PSU) [10]. A brief summary of these works is provided next. A series of studies (1994-2003) in five configurations were carried out at the University of Santa Barbara. In 1994, Theofanous et al. [4] carried out an experiment on the ULPU facility for the lowermost spherical segment of the RPV. Stainless steel was used as a heater material and a correlation was developed for prediction of the CHF. Later Theofanous and Syri [5] extended the study to SA508, the actual RPV material. The CHF values for SA508 were higher than those for stainless steel. However, it was not clear whether the CHF difference resulted from the heater material or thermal inertia effects because different test sections from these studies had significantly different heater thicknesses. In 2003, Dinh et al. [6] carried out a more complete set of experimental data which covered different mass fluxes and inclination angles on the same ULPU facility, but again stainless steel and copper were used as the heater materials and the term "aging" was used by the authors to capture the effect of surface characteristics on CHF.

The SULTAN facility [7] was a forced convection experiment facility and their experimental data covered a wide range of mass fluxes, pressures, subcooling and inclination angles relevant to IVR. Stainless steel was used in this study as the heater material.

Asfia and Dhir at UCLA [8] measured the natural convection heat transfer coefficient on the outer surface of a hemispherical heater, and found that the heat transfer coefficient was lowest at the bottom of the heater and increased with the polar angle along the spherical segment of the test section.

Yang et al. at PSU [10] conducted a series experiments on a stainless steel heater to investigate the effect of surface coating on transient quenching and steady-state boiling. The CHF value for the aluminum coated surface was much higher in comparison to the corresponding data without coating.

Recently Jeong et al. [11] measured the CHF of a two-dimensional slice test section made of stainless steel grade 304. The tests were conducted at various inlet subcooling and mass fluxes. The measured CHF data from this study was slightly lower than the ones measured in UCSB experiment [5]. The proposed reason for the observed trend was the difference in test section material and thickness (different thermal inertia). Park et al. [12] also executed a CHF experiment with a test section in which they varied the radius of curvature, the width and gap size. The results from this experiment were in good agreement with Jeong et al. [11] data, as the

same heater material was used in both studies. DeWitt et al. [13] measured the CHF of nanofluids (water + 0.001$Vol\%$ alumina) for the geometry and flow conditions relevant to IVR, using a stainless steel surface, and found an average enhancement of 70% in CHF with respect to the pure water case.

It is interesting to note that, in all previous IVR CHF studies (except the one by Theofanous and Syri [5]) the boiling surface material was stainless steel. However, the reactor pressure vessel (RPV) is made of low carbon steel and its surface has a relatively thick oxide layer that results from pre-service heat treatment and oxidation during service. This oxide layer introduces significant differences in surface wettability, porosity, and roughness in comparison to an un-oxidized stainless steel surface, which affect CHF.

Very recently, the effect of heater material on CHF was considered by Park et al. [14] who used downward facing curved heaters made of stainless steel grade 304 and SA508. For all the test conditions the CHF values were higher for SA508 in comparison to stainless steel. Oxidation of carbon steel in the aqueous environment was proposed as a reason for the enhancement of the CHF.

All of these studies suggest the importance of measuring CHF with a heater having surface characteristics as close as possible to the actual outer surface of the RPV. In this paper a systematic study to examine the effect of surface characteristics of low carbon steel surfaces is presented. Specifically, test heaters were fabricated out of RPV low carbon steel, pre-oxidized in a controlled high temperature environment, emulating the surface oxides present on the outer surface of the actual RPV; the heaters were then tested in a flow boiling loop designed specifically for the IVR conditions.

2. Experimental Method
2.1. Facility

Figure 1 presents a schematic diagram of the two phase flow loop facility that was used for flow boiling CHF measurements in this study. Reference [15] provides extensive details of the experimental apparatus used here. Briefly, the experimental setup is a closed loop flow system equipped with a centrifugal pump, flow meter, pre-heater, test section, accumulator, and condenser. The test section in the flow system is made of stainless steel 316. The rectangular flow channel is 1.4 cm wide, 2 cm deep, and 31.7 cm long. Characteristics of the test section were designed to be hydro-dynamically similar to the vessel/insulation gap in an AP1000 through scaling analysis which can be found in Reference [15]. The test section was designed to have single sided downward facing heating and the flexibility to be mounted at different angles from vertical (90°) to horizontal (0°). The test heaters are resistively heated flat plates with studs at each end to provide a connection for DC electrodes, attached to two 18 kW DC power supplies operated in parallel. The joule heated test heater is 1 cm wide and 24 cm total length in size (Figure 2). A 2-hp centrifugal pump was used to circulate the working fluid in the loop. The pump is appropriate for temperatures up to 180 ^{o}C with a low net positive suction head. A turbine type flow meter is utilized on the experimental apparatus to measure the mass flow rate in the range of 165 to 1,651 kg/m^{2}s. A 2 kW pre-heater was also implemented to control the test

section inlet temperature as shown in Figure 1. An accumulator was used to accommodate volumetric expansion of the working fluid during heating. A shell and tube heat exchanger was used to reject the heat. A data acquisition system was employed to record the output of all instruments. Calibrations were completed for all the measurement devices. The error on the measured CHF is estimated to be 4%, based on propagation of the uncertainty of the instruments used.
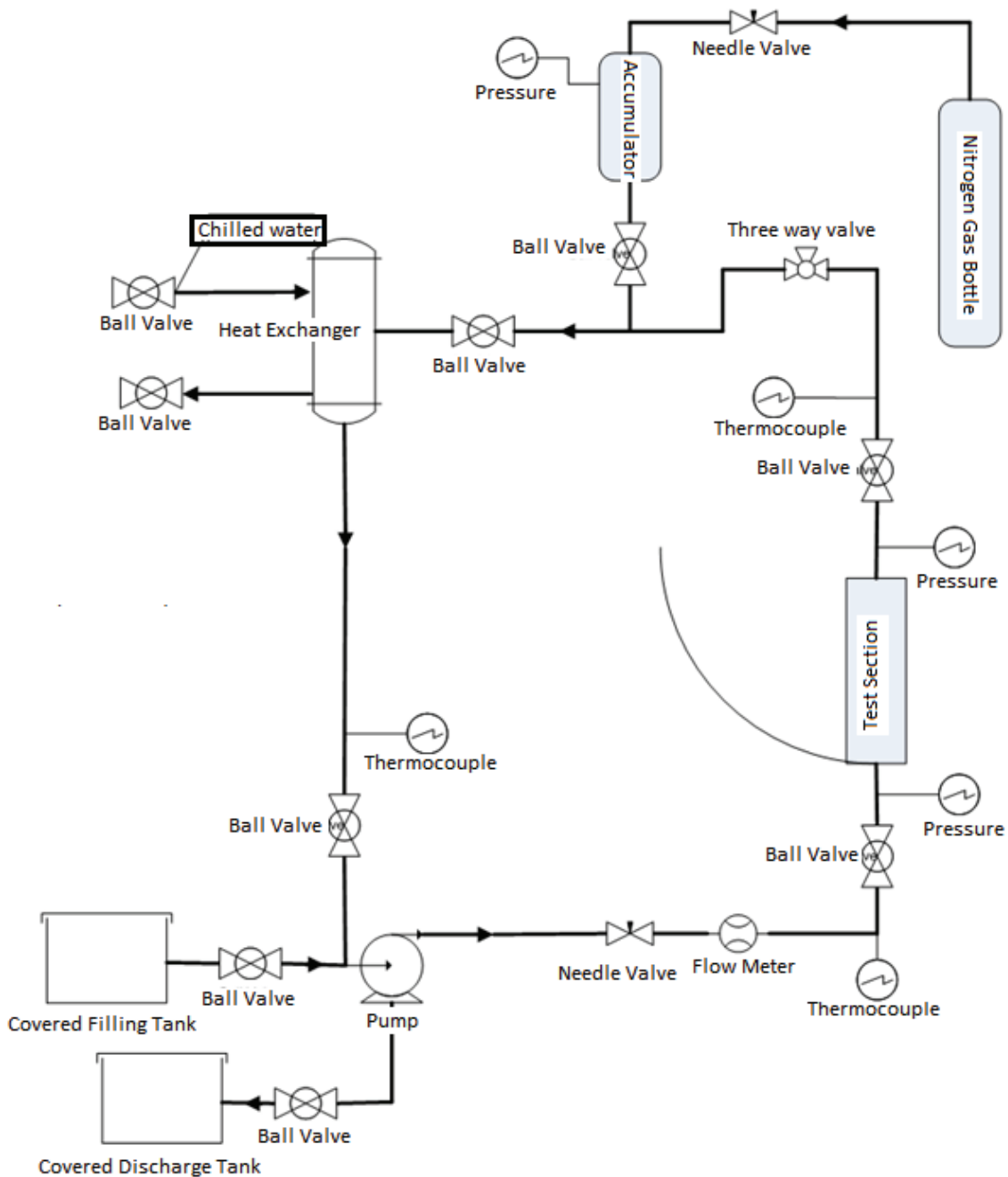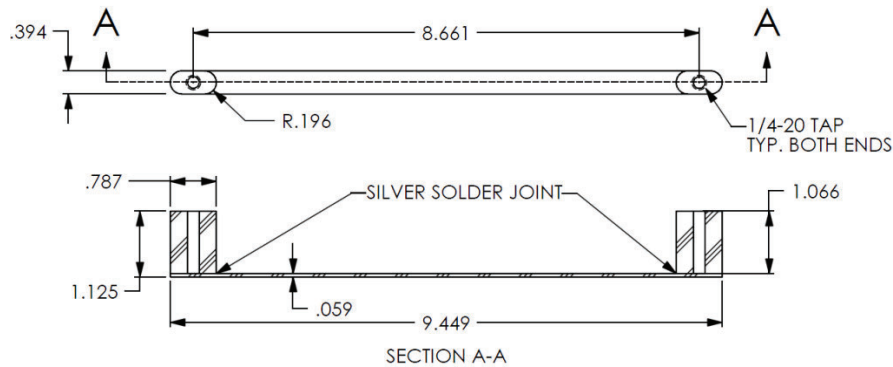

Figure 1. MIT CHF flow loop [15]

Figure 2. Schematic of the heater with wetted surface facing down (dimensions are in inch); heated length equals 20 cm.

2.2. Heater preparation

Two materials were tested in this study: stainless steel grade 316 (SS316) and low carbon steel (18MnD5). The heaters were categorized in two groups unoxidized heaters (i.e. SS316 and 18MnD5 without any oxidation) and oxidized ones (oxidized 18MnD5). Before CHF test or any oxidation, heaters were sandblasted and cleaned with deionized water, acetone and ethanol. Controlled oxidation was performed in an oxidation facility (Figure 3).
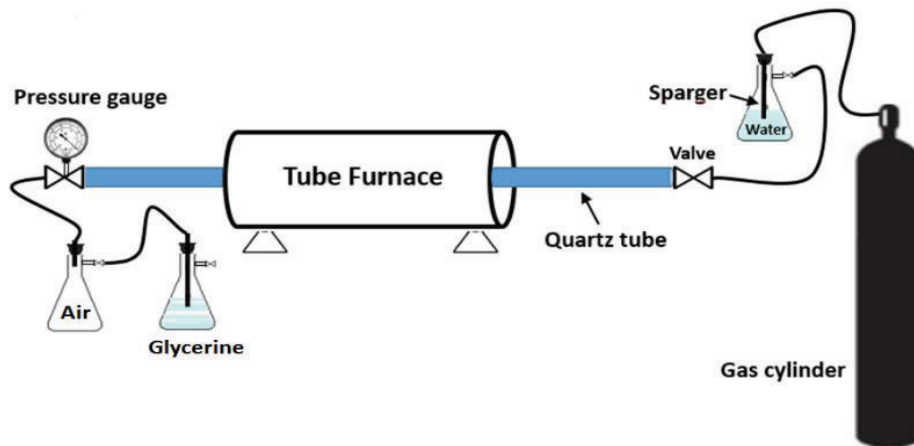

Figure 3. Oxidation facility used in this study.

The synthetic air (AI B300) provided by Airgas Inc. is used for oxidation. The air was sparged through a room-temperature water flask to establish a controlled 3% vol. humidity of the air prior to delivery to the tube furnace. Some humidity is needed to increase the adhesive properties of the oxide layer [16]. The temperature of the furnace was set to 625 ± 10 $^{\circ}$C for 8 hours. A representative temperature track for one of the oxidized heaters is shown in Figure 4. Temperature was ramped up to 625 $^{\circ}$C and held constant for 8 hours prior to the cooling down process.
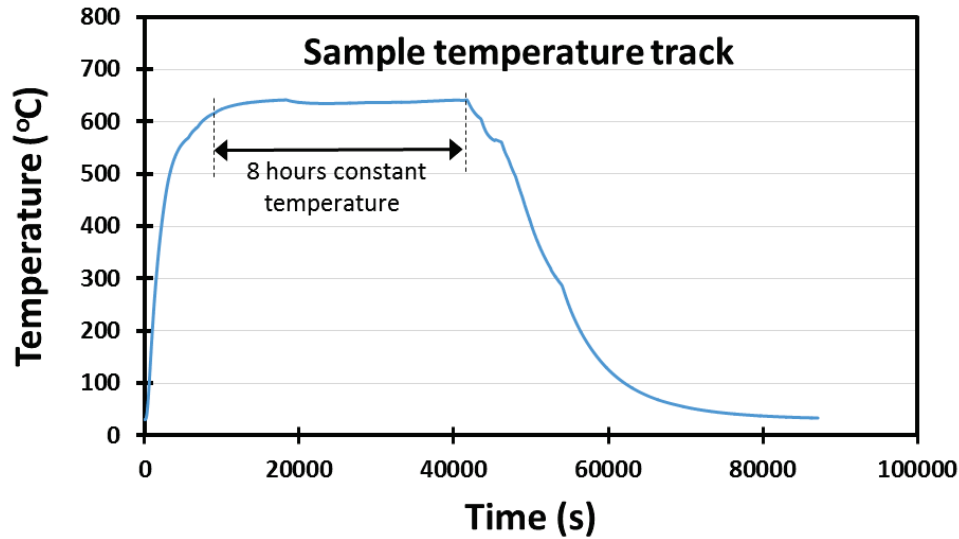
Figure 4. Temperature track of an oxidized heater (8 hours oxidation treatment).

3. Results and discussion

3.1. Oxidation and surface characterization

Low carbon steel (18MnD5) was selected for the purpose of this study as 18MnD5 is the French alloy used in the fabrication of RPVs. SA508 is the alloy used in the US for RPVs. Table 1 shows the chemical composition of SA508 and 18MnD5. Clearly both materials have a very similar chemical composition.

Table 1. Chemical composition of 18MnD5 as well as SA508 (MMR group, Inc.)

Chemical composition	C	Mn	Ni	Mo	P	S	Si	Cr
18MnD5	0.2	1.51	0.6	0.46	<0.01	0.003	0.26	0.22
SA508	0.21	1.29	0.59	0.56	0.014	0.014	0.3	0.05

Oxidation of 18MnD5 heaters was carried out with a furnace as explained in the last section. Oxide layers as thick as 40 µm were fabricated in this experiment. While the oxidation behavior of low carbon steel is expected to be similar to that of pure iron [17], the microstructure of the oxide layer could be very complex and is dependent on the heat treatment, oxidation environment, and alloying elements present in the steel. From the iron-oxygen phase diagram (Figure 5) it is clear that above 570°C there are three stable oxide phases, i.e. Wüstite (FeO), magnetite (Fe_3O_4) and hematite (Fe_2O_3). After a very thin layer of oxide is formed, the kinetics of oxidation will be controlled by outward diffusion of iron atoms and inward diffusion of oxygen atoms through that oxide layer. Therefore, oxide layers on the steel surface generally have a layer of Wüstite (FeO) closest to the substrate with the lowest oxygen content, an intermediate magnetite layer (Fe_3O_4) and a final oxygen-rich thin hematite layer (Fe_2O_3) [18]. X-ray diffraction analysis was carried out for the oxidized heaters (Figure 6). It can be seen that the peaks match well with the XRD patterns of magnetite and hematite which confirms their existence.
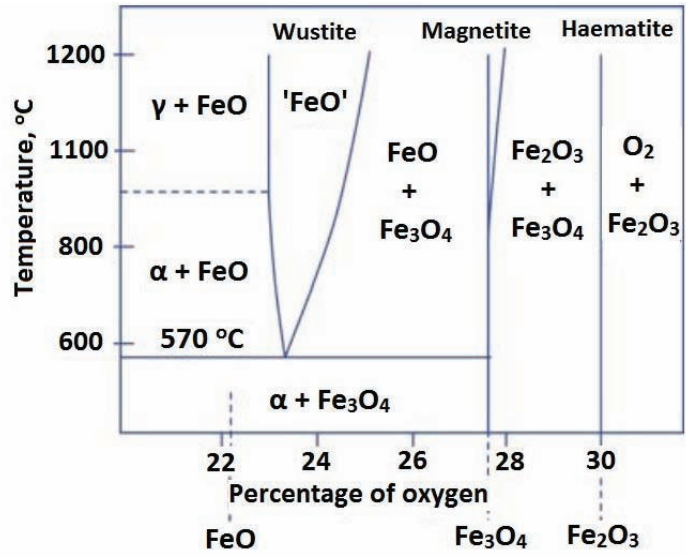
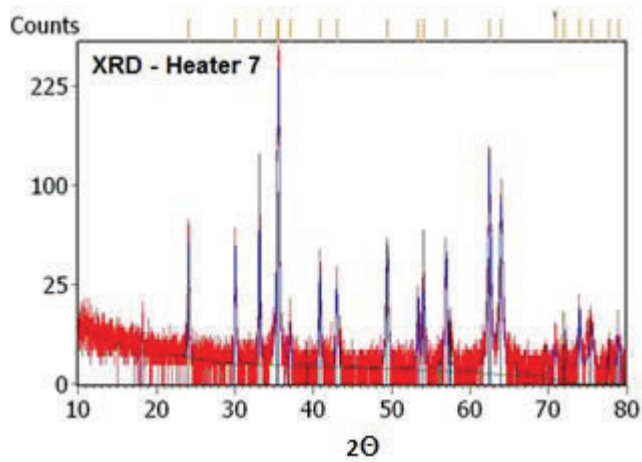Figure 5. Iron-Oxygen phase diagram [19]

Figure 6. XRD pattern of an oxidized heater.

The appearance of the unoxidized 18MnD5 heater after sand blasting and oxidized heater after oxidation is shown in Figure 7. The oxidation was quite uniform and adherent for the oxidized heaters.
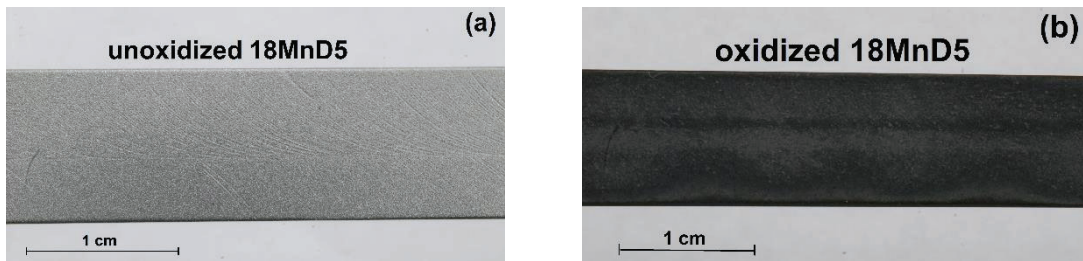

Figure 7. (a) Unoxidized and (b) oxidized heater appearance.

Surface properties are crucial in determining the boiling heat transfer performance of the system. One of the key surface properties in boiling is wettability of the surface of interest. Static contact angle of the surface is representative of the surface wettability and can be measured by a contact angle goniometer setup. Contact angle measurement was executed for all heaters in this study. Contact angle measurements of an unoxidized 18MnD5 heater compared to the oxidized heaters show a reduction of contact angle from 45 degrees to zero (Figure 8 (a) and (b)). This observation suggests that the surface after oxidation becomes super-hydrophilic. In fact, all the treated heaters in this study were super-hydrophilic. For SS316 the contact angle drops from 85 degrees before CHF test to 25 degrees after the CHF test. The contact angle of unoxidized 18MnD5 was also dropped from 45 degrees before CHF test to 5 degrees after the test (due to oxidation during the CHF test).
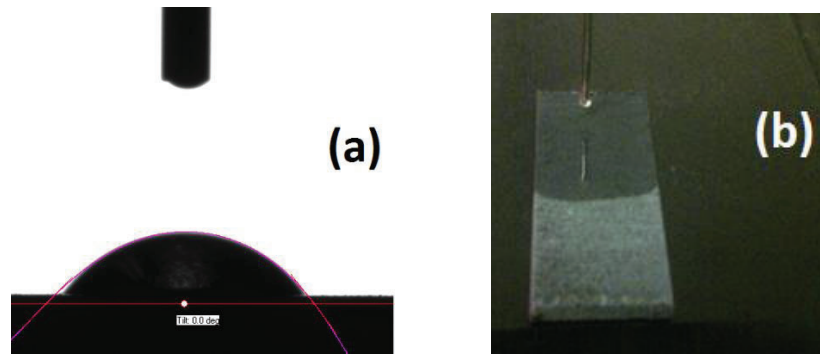

Figure 8. Contact angle measurement on (a) unoxidized 18MnD5, (b) oxidized 18MnD5 (8 hrs DO)

To develop a better understanding of the surface characterization for each heater, scanning electron microscopy (SEM) images were acquired before and after CHF test (Figure 9).
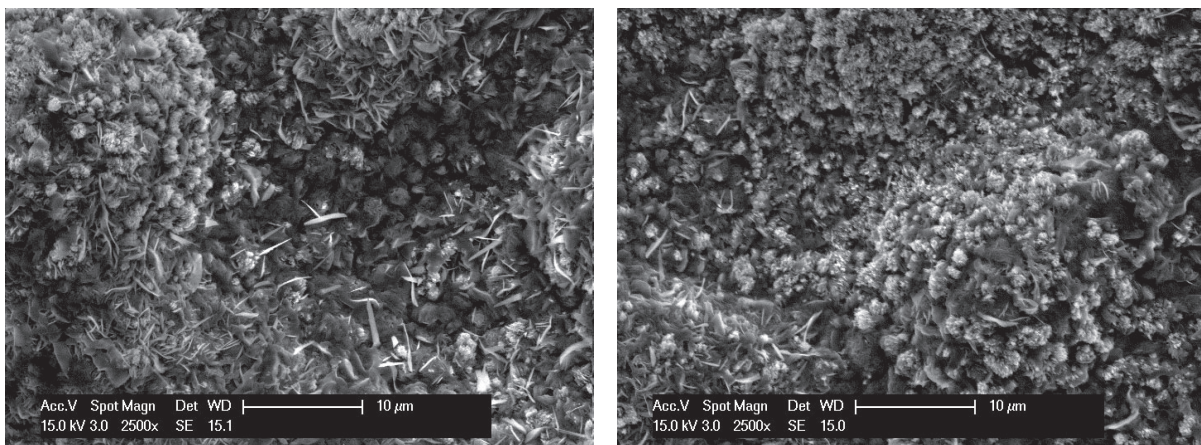

Figure 9. SEM image of the oxidized heater before (left) and after (right) the CHF test.

The surface structure of an oxidized 18MnD5 sample was flowery (whisker-like), Figure 9. It can also be seen in Figure 9 that the texture of the surface was unchanged by the CHF testing. The oxidation thickness was also measured by SEM. Heaters are cut and mounted in epoxy and prepared for oxidation thickness measurement. Figure 10 shows the oxidation thickness for an oxidized heater. Figure 10(a) shows the SEM image of the oxidized low carbon steel cross

section (40 μm). Energy dispersive X-ray spectroscopy (EDS) was also executed on our oxidized heater for elemental analysis. Figure 10(b) shows an EDS line scan data. It is clear that the iron concentration is much higher in the 18MnD5 side of the heater, and that in the oxide layer the oxygen concentration increases and both (iron and oxygen elements) drop in the epoxy (light gray region).
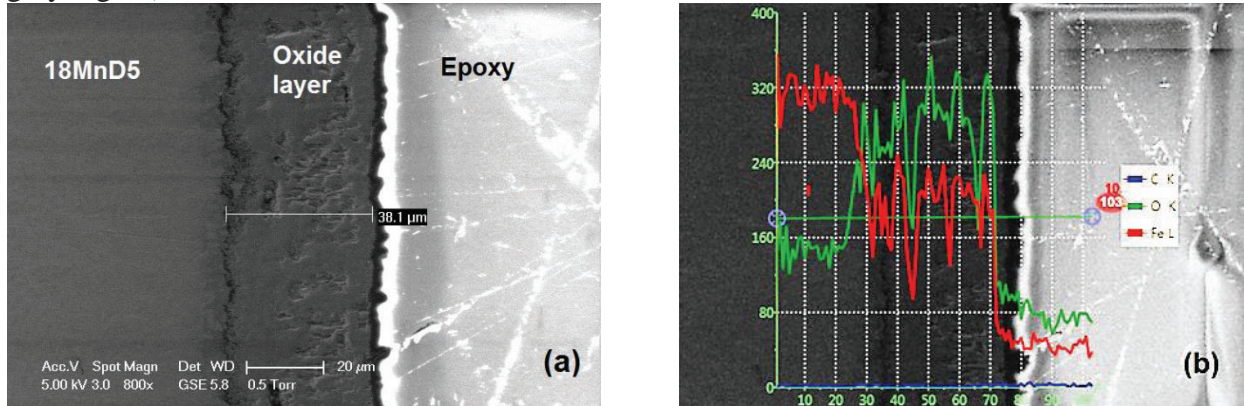

Figure 10. (a) SEM image of the oxidized heater crossed section, and (b) EDS analysis of the oxidation thickness.

3.2. Critical Heat Flux Test

Two test conditions were chosen for the CHF tests:
- Test condition I: 90 degrees (vertical) test section, 500 kg/m^{2}s mass flux, 7 degree subcooled, and atmospheric pressure.
- Test condition II: 45 degrees test section, 1000 kg/m^{2}s mass flux, saturation temperature, and atmospheric pressure.

For each test condition, a given heater material and surface state was tested twice, for repeatability.

The experiments were carried out in a quasi-steady state manner with incremental power changes, and with time provided between each step for the system to reach equilibrium. An example of the power history for a test is shown in Figure 11. Electrical resistance of the heaters is measured as the DC power supplies are operated in constant current mode. The sharp reduction in heat transfer at CHF causes a fast increase in sample temperature. Since the electrical resistivity of steel increases with temperature, CHF results in a large and sudden increase in the heater resistance and therefore heat flux. Nearly all of the CHF tests run ended with heater failure due to the thermal stresses. The average of three values of the heat flux, right before the sudden increase in the heater resistance, is reported as the CHF value for that test. These three values are shown in Table 2 as an example for one of the treated heaters under the test condition I (i.e. 500 kg/m^{2}s mass flux, vertical test section and 7 degree subcooled).
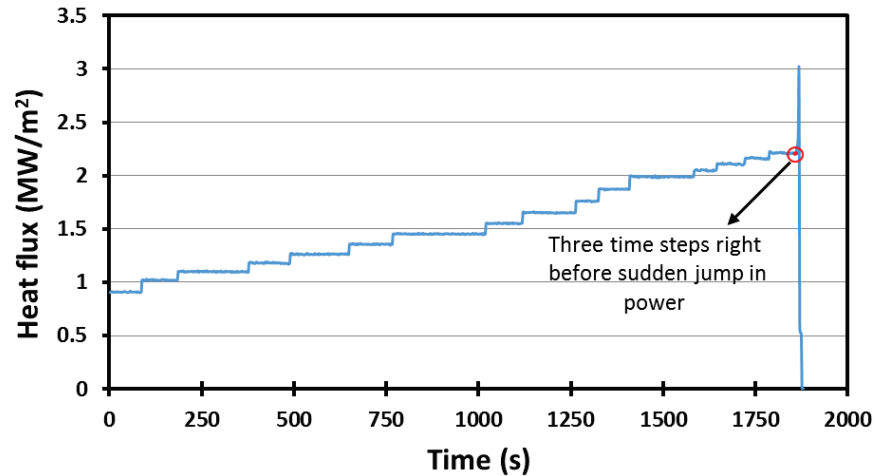
Figure 11. Power increment versus time for one of the treated heaters.

Table 2. Data for three time steps just before CHF for one of the treated heaters under test condition I (90°, 500 kg/m²s, 7°C sub).

Time points just prior to CHF (s)	Exit Pressure [Bar]	Mass flux [kg/m²s]	Test section angle	T_{sat} @ Exit [C]	T_{out} bulk [C]	T_{in} bulk [C]	Exit quality	CHF value [MW/m²]	T_{sat} - T_{in}	T_{sat} - T_{out}
6	0.97	573	90	98.62	93.92	87.67	-0.00851	2.21	10.95	4.70
4	1.09	536	90	101.95	93.91	87.66	-0.01396	2.21	14.29	8.05
2	1.04	586	90	100.55	93.91	87.66	-0.01241	2.21	12.89	6.64
Average	1.03	565	90.0	100.37	93.91	87.66	-0.01163	2.21	12.71	6.46

CHF values for different oxidized/unoxidized heaters are shown in Table 3 and Figure 12.

Table 3. CHF data for various conditions and heaters

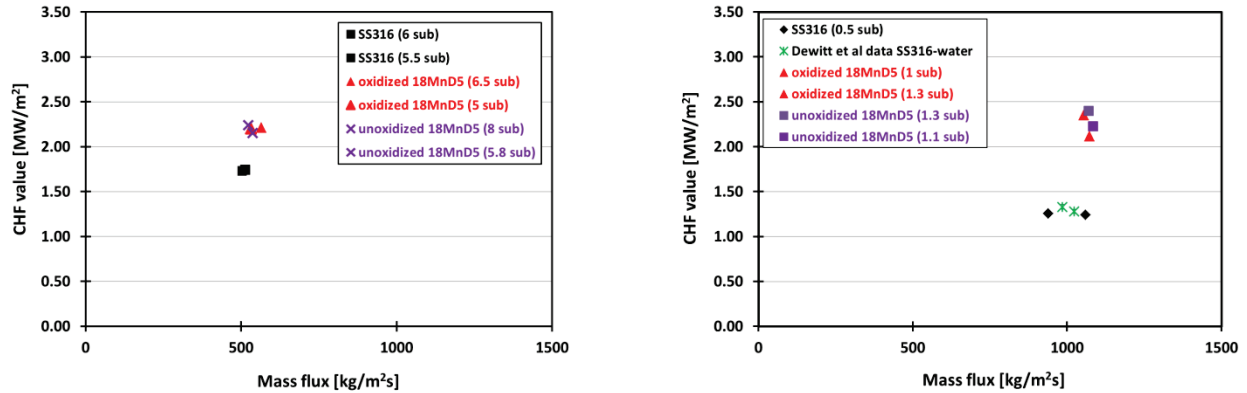| Heater	CHF (MW/m2) 90°, 500 kg/m²s, 7°C sub	CHF (MW/m2) 45°, 1000 kg/m²s, sat
SS 316	1.73	1.24
SS 316	1.74	1.26
18MnD5 (unoxidized)	2.15	2.4
18MnD5 (unoxidized)	2.24	2.23
18MnD5 (oxidized)	2.21	2.12
18MnD5 (oxidized)	2.20	2.35

Figure 12. CHF data for test condition I (90°, 500 kg/m^{2}s, 7°C sub) (left), and test condition II (45°, 1000 kg/m^{2}s, sat) (right).

It is clear that there is an enhancement in CHF value for the case of oxidized as well as unoxidized 18MnD5 in comparison to SS316. Up to 30% and 70% enhancement in CHF value was observed in the case of oxidized 18MnD5 in comparison to SS316 for test condition I and II respectively. The hydrophilic structure of the oxide on top of the heater is proposed as a reason for the observed enhancement in CHF value. Future work will determine the porosity of these surfaces to investigate the influence of capillary wicking. In the case of unoxidized 18MnD5 enhancement in CHF was up to 27% in comparison to SS316 under the test condition I which is quite similar to 30% in the case of oxidized 18MnD5. Same behavior was observed for the test condition II. Post-CHF SEM image of unoxidized 18MnD5 reveals a presence of a porous structure, with the thickness of a few microns (Figure 13). This observation along with a measured super-hydrophilic nature of the post-test surface provides a plausible explanation for the observed enhancement of CHF value even in the case of unoxidized 18MnD5 [1].
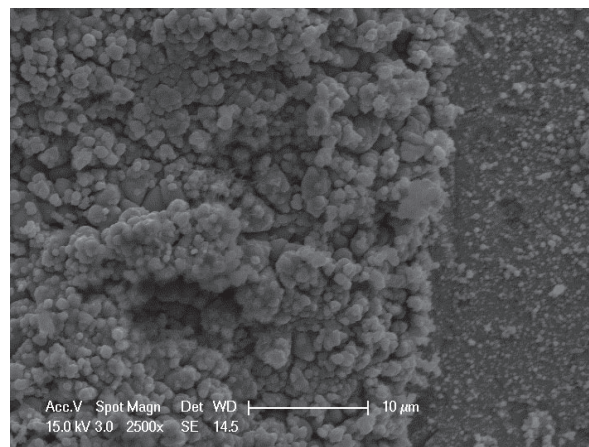

Figure 13. Post-CHF SEM image of the surface for an unoxidized 18MnD5.

This analysis confirms that the initially unoxidized 18MnD5 surface was modified during boiling, likely from oxidation by water. The same observation was made for SA508 [13]. Ref. [20] reports that application of a current to low carbon steel in contact with water causes electrochemical oxidation of the steel surface.

4. Conclusion

Effect of surface oxidation on flow boiling CHF value was determined in this study. It has been shown that the flow boiling CHF value can be enhanced by altering the surface characteristics through oxidation (both through pre-oxidation and oxidation during the test). Low carbon steel was oxidized in a controlled environment. This surface is very similar to the one in RPV during the IVR scenarios. Two test conditions were selected for the purpose of this study. Test condition I: 90 degrees (vertical) test section, 500 kg/m^{2}s mass flux, 7 degree subcooled, and atmospheric pressure, and test condition II: 45 degrees test section, 1000 kg/m^{2}s mass flux, saturation temperature, and atmospheric pressure. Up to 30% and 70% enhancement in CHF value was observed in the case of oxidized 18MnD5 in comparison to SS316 for test condition I and II respectively. Superhydrophilic properties of the surface is proposed as the main reason for the observed enhancement. It was also observed that even in the case of unoxidized 18MnD5 the heaters were oxidized during the experiment. Post-CHF SEM image reveals the formation of a few micron thick oxidation on the surface of heater. This surface change leads to 27% enhancement in CHF value for the case of unoxidized 18MnD5 in comparison to SS316 under the test condition I. This observation clearly shows that although oxidation enhances CHF value by altering the surface characteristics, the oxidation thickness, in the range studied here, is not an important factor.

References

[1]   O'Hanley, H., Coyle, C., Buongiorno, J., McKrell, T., Hu, L-W., Rubner, M., Cohen, R., 2013, "Separate effects of surface roughness, wettability, and porosity on the boiling critical heat flux", *Applied Physics Letters*, 103, pp. 024102.

[2]   Kim, H., 2011, "Enhancement of critical heat flux in nucleate boiling of nanofluids: a state-of-art review", *Nanoscale Res Lett.* 6 (**1**) 415.

[3]   Kandlikar, S.G., 2001, "Critical heat flux in subcooled flow boiling – an assessment of current understanding and future directions for research", *Multiphase Science and Technology*, 13 (**3**), pp. 207-232.

[4]   Theofanous, T.G., Syri, S., Salmassi, T., Kymalainen, O., Tuomisto, H., 1994, "Critical heat flux through curved, downward facing, thick walls", *Nuclear Engineering and Design*, 151, pp. 247-258.

[5]   Theofanous, T.G., Syri, S., 1997, "The coolability limits of a reactor pressure vessel lower head", *Nuclear Engineering and Design*, 169, pp. 59-76.

[6]   Dinh, T-N., Tu, J.P., Salmassi, T., Theofanous, T.G., "Limits of coolability in the AP1000 related ULPU-2400 configuration V facility", University of California, Santa Barbara, CRSS- 03/06, June 30, 2003.

[7]   Rouge, S., Dor, I., Geffraye, G., "Reactor Vessel External Cooling for Corium Retention SULTAN experimental program and modeling with CATHARE code", Workshop on in-vessel core debris retention and coolability, Garching, Germany, 3-6 March, 1998.

[8]   Asfia, F.J., Dhir, V.K., 1996, "An experimental study of natural convection in a volumetrically heated spherical pool bounded on top with a rigid wall", *Nuclear Engineering and Design*, 163, pp. 333-348.

[9]   Chu, T., Bentz, J., Simpson, R., 1995, "Observations of the Boiling Process from a Downward-Facing Torispherical Surface: Confirmatory Testing of the Heavy Water New

Production Reactor Flooded Cavity Design", Sandia National Laboratory, Presentation at the 30th National Heat Transfer Conference, Portland, Oregon, August 5-9, 1995.

[10] Yang, J., Dizon, M.B., Cheung, F.B., Rempe, J.L., Suh, K.Y., Kim, S.B., 2006, "CHF enhancement by vessel coating for external reactor vessel cooling", *Nuclear Engineering and Design*, 236, pp. 1089-1098.

[11] Jeong, Y.H., Chang, S.H., 2004, "Critical heat flux experiments on the reactor vessel wall using 2-D slice test section", *Nuclear Technology*, 152, pp. 162-169.

[12] Park, H.M., Jeong, Y.H., Heo, S., 2013, "The effect of the geometric scale on the critical heat flux for the top of the reactor vessel lower head", *Nuclear Engineering and Design*, 258, pp. 176-183.

[13] Dewitt, G., McKrell, T., Buongiorno, J., Hu, L-W., Park, R.J., 2012, "Experimental study of critical heat flux with alumina-water nanofluids in downward-facing channels for in-vessel retention applications", *Nuclear Engineering and Technology*, 45 (**3**), pp. 335-346.

[14] Park, H.M., Jeong, Y.H., Heo, S., 2014, "Effect of heater material and coolant additives on CHF for a downward facing curved surface", *Nuclear Engineering and Design*, 278, pp. 344-351.

[15] DeWitt, G.L., "Investigation of Downward Facing Critical Heat Flux with Water-Based Nanofluids for In-Vessel Retention Applications", *Ph.D. Thesis*, Nuclear Science and Engineering Department, MIT, September 2011.

[16] Baud, J., Ferrier, A., Manenc, J., Benard, J., 1975, "The oxidation and Decarburizing of Fe-C Alloys in Air and the Influence of Relative Humidity", *Oxidation of Metals*, 95, pp.69-97.

[17] Khanna, A.S., "High temperature oxidation", Handbook of Environmental Degradation of Materials, Williams Andrews Publication (2005) pp. 105-152.

[18] Birosca, S., West, G.D., Higginson, R.L., "Microstructural investigation of the oxide scale on low carbon steel", *14th International Metallurgical & Materials-Metal proceedings*, pp. 73, Tanger, Ostrava, Czech Republic, 2005.

[19] Lide, D.R., *Hand book of Chemistry and Physics*, CRC Press, New York, USA, 88th edn. 2007-2008.

[20] U.S. Department of Energy, 1993. DOE-HDBK-1015/1-93, DOE Fundamentals Handbook: Chemistry, Volume 1 of 2. U.S. Department of Energy, Washington, DC.